Efficient Modelling of a Nonlinear Gust Loads Process for Uncertainty Quantification of Highly Flexible Aircraft

R. G. Cook*, C. J. A. Wales*, A. L. Gaitonde†, D. P. Jones†, J. E. Cooper‡

University of Bristol, Queen's Building, University Walk, Bristol, BS8 1TR, United Kingdom

An efficient gust loads process is presented which can predict worst case loads on a highly flexible aircraft, for use in uncertainty quantification. This process generates a neural network surrogate model of an aeroelastic system using linearised system equations to rapidly determine worst gust cases, including the capability to model atypical gust excitations. The surrogate model is used to produce a reduced set of identified gust cases which cause the largest loads; these cases are then run in the nonlinear code. Uncertainty quantification of this gust process is carried out using polynomial chaos expansion (PCE) techniques, considering uncertain structural properties. Convergence studies of the gust loads using PCE indicate significantly fewer samples are required than would be for a Monte Carlo simulation. It is demonstrated how oblique gusts exceed the loads envelope from a traditional gust process, justifying the need to consider alternative gust excitations, but interestingly for the particular test case in this work, uncertain structural properties can be seen to have little effect on the uncertainty of the static 1g and gust loads.

Nomenclature

1MC	1-minus-cosine
H	Gust Gradient (Half Gust Length) (m)
HAR	High-Aspect-Ratio
HTP	Horizontal Tail Plane
ϕ	Oblique Gust Angle (°)
IQs	Interesting Quantities
μ	Mean Value
MCS	Monte Carlo Simulation
PC(E)	Polynomial Chaos (Expansion)
PDF	Probability Density Function
RTC	Round-the-Clock
σ	Standard Deviation
θ	Round-the-Clock Gust Angle (°)
UQ	Uncertainty Quantification
VTP	Vertical Tail Plane

I. Introduction

One approach that aircraft designers can adopt to reduce CO_2 emissions or increase aircraft range, and help to meet environmental targets outlined in Flightpath 2050,[1] is to consider high-aspect ratio (HAR) aircraft. Such slender-winged planes have potential to exhibit significantly higher lift-to-drag ratios compared to traditional aircraft thanks to reduced lift-induced drag components, but with added complications that

*Research Associate, Department of Aerospace Engineering (Project Website: `https://aerogust.eu`)

†Reader in Aerodynamics, Department of Aerospace Engineering

‡Royal Academy of Engineering Airbus Sir George White Professor of Aerospace Engineering, AFAIAA, Department of Aerospace Engineering

manifest in the form of structural nonlinearities and strong rigid-body to flexible mode coupling. As a result, the techniques used in industry standard processes, typically assuming a linear system, may no longer be appropriate for such a class of aircraft. Therefore, it is becoming increasingly important to be able to analyse nonlinear aircraft in a rapid and efficient manner such that well-defined, traditional industrial approaches to aircraft design can still be modified and applied. An important aspect of aeroelastic analysis of an aircraft, and the focus of the work in this paper, is the modelling and prediction of structural loads due to atmospheric gust excitations. Previous work has considered methods to reproduce gust loads using surrogate models[2] where numerous mass and flight cases can be considered. However, in that work only linear models were considered, which would not model important effects associated with highly flexible structures.

Further to modelling the gust loads of a highly-flexible aircraft, it is increasingly important to understand how uncertainties in the manufacturing or modelling process might affect interesting quantities (IQs); it may not be possible to know particular system parameters with exact certainty. The work in this paper will consider creating surrogate models of a gust loads process in order to carry out an uncertainty quantification (UQ) analysis of a highly flexible aircraft in a relatively short time frame. In the following sections, the efficient gust load process, and uncertainty quantification approaches will be outlined, followed by description of a test case, results, and conclusions.

II. Methodology

At the heart of the uncertainty quantification (UQ) analysis in this work is a low state-size aeroelastic solver. This must be capable of capturing the nonlinear structural effects that are anticipated from high AR aircraft, but with small computational cost. An efficient gust loads process is then needed, which uses numerous aeroelastic analyses to identify a subset of all anticipated gust excitations without excessive numbers of simulations. Finally, an uncertainty quantification approach is described which calls multiple gust loads processes to determine statistical information of the output IQs subject to uncertain inputs. In this section, the whole procedure is described in stages. First, the aeroelastic solver is presented, followed by the gust loads process, and finally the uncertainty analysis.

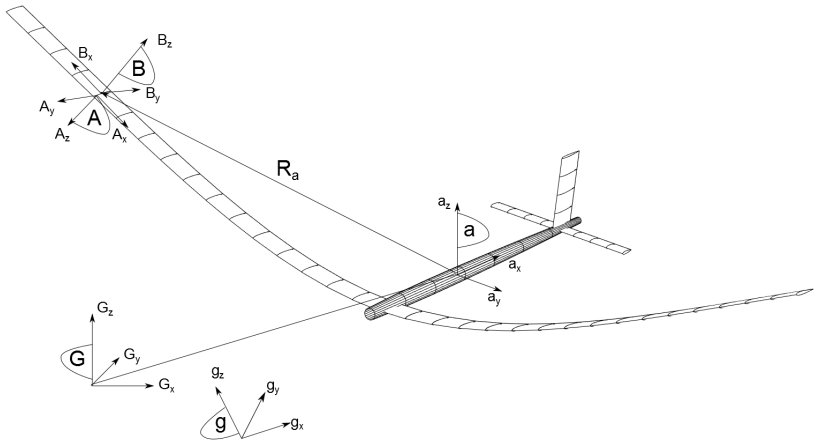

Figure 1: An illustration of a highly flexible aircraft in a trim flight shape.

A. Nonlinear Aeroelastic Modelling

The nonlinear aeroelastic modelling approach used in this work is described briefly here. The particular method used in this work has been described in more detail in previous work.[3]

1. *Nonlinear Structural Modelling*

The structural portion of the aeroelastic solver is modelled using a geometrically-exact, intrinsic beam formulation, described in detail by Hodges;[4] the various members of the aircraft are modelled as a free-free collection of interconnected beams. Such beam representations of aircraft models are justified for low-order modelling of an aircraft structure, particularly when considering very slender structures as in this work where chord-wise deformations are significantly smaller than span-wise ones. An example of such a flexible aircraft is illustrated in Fig. 1.

The implementation of this method is similar to that used in Hodges *et al*,[5] where piecewise-linear finite-elements are used to discretise the intrinsic beam PDEs. In this approach however, the intrinsic beam equations are solved directly, rather than using a mixed formulation as in Hodges *et al*;[5] positions and orientations of the beam are procured as either a spatial integration of the beam shears and curvatures, or as temporal integration of the velocities (with quaternions used for the orientation integration).

2. *Unsteady Aerodynamics*

The aerodynamics model comes from an unsteady, thin-aerofoil strip theory method, using Leishman's indicial response method.[6] In this solver, Jones' rational function approximation (RFA) of Theodorsen's function[7] is used to cast the frequency-domain aerodynamics into the time-domain. Three-dimensional effects are included into the formulation by using lift-curve slopes from a standard vortex-lattice method solver about an undeformed geometry. At least for static results, it was shown in previous work[8] how this approach is justified even for large deformations. The linear assumptions of this approach mean there is no inherent capability to capture transonic or separation effects; compressibility effects will also be ignored (Mach number will be set to zero).

3. *Numerical Implementation*

The coupled nonlinear structural and unsteady aerodynamics models are implemented in MATLAB. The static solver is a Newton-Raphson based iterative scheme, and the trim solver is an additional Newton-Raphson solver wrapped around the static solver to determine angle of attack and elevator deflections to balance total global forces and moments on the aircraft.

The nonlinear equations are linearised analytically to produce a linear state-space system which can be quickly simulated using MATLAB's in-built *lsim* solver. Linear model reduction techniques using modal truncation are used to remove exceptionally high-frequency modes and reduce the state-size of the problem.

The full nonlinear equations are solved using a Newmark-β solver, based on the work of Shearer and Cesnik.[9]

B. Gust Loads Processes for Nonlinear Aeroelastic Systems

In order to determine the worst case loads that an aircraft might experience in-flight, regulatory bodies[10,11] define representations of atmospheric excitations which should give the largest loading. In short, they define either discrete gusts (in the form of 1-cosine (1MC) distribution) or continuous gusts (described using the von Kármán spectrum); the former of the two is considered in this work.

When considering 1MC discrete gusts, the regulations state that a 'sufficient'[10,11] number of gust lengths need to be run to ensure the worst length has been captured. Further to this, vertical and lateral gusts should be considered to ensure that round-the-clock (RTC) gusts (a combination of vertical and lateral gusts) do not exceed the envelope of a purely vertical or lateral gust. Typically on conventional aircraft, RTC loads only exceed the loads from a vertical of lateral gust on components like engines and pylons or T-tails[12] where lateral and vertical gust excitations can both exert significant loading. However, as seen in previous work, aircraft which exhibit large structural deformations can also see worst case excitations due to off-vertical gusts.[3]

For linear systems, running large numbers of gust loads is achievable due to model reduction techniques, such as modal representations. These approaches which drastically reducing state size, in conjunction with superposition principles, mean that fewer, less computationally intensive simulations need to be run. For example, only vertical and lateral gusts need to be considered, as negative and RTC gust loads can be determined as a post-process. In contrast, a nonlinear system cannot be analysed in such a way; highly flexible aircraft represent a huge challenge for efficient gust loads analysis due to more computationally

expensive nonlinear solutions combined with a requirement for more simulations to be run (superposition can no longer be assumed).

1. *Consideration of Atypical Gust Excitations*

The typical gust excitations described previously are considered to be sufficient for conventional aircraft designs, but as faster, larger and higher-aspect ratio aircraft begin to be considered, it is essential to adapt the gusts as defined in the regulations. This effect has been demonstrated recently with the introduction of the Airbus A380, and the resulting changes made in the analysis to accommodate it.[13]

One consideration that should be made for aircraft with large wingspans is span-wise-varying and asymmetric gusts. Whereas the regulations assume the gust is span-wise uniform and aligned normal to the flight direction, this may not be a true representation of a gust if the aircraft span is comparable to the length scales of turbulence.

Numerous authors have considered atypical excitations in their analyses. For example, Houbolt[14,15] considered the effect of span-wise turbulence an addition to the typical, remarking that it provided a more appropriate model of the atmosphere. DARPA[16] document how a cosine velocity distribution in the span-wise direction should be considered into the analysis of their Vulture II aircraft.

In this work, an asymmetric gust excitation will be considered in the form of a so-called oblique gust. In this gust excitation, the 1MC discrete gusts are still considered, but with the added possibility of hitting the gust at an oblique angle, rather than normal to the flight direction, as in a traditional gust loads analysis. An example of such a gust is shown in Fig. 2 in a top down view, where the oblique gust angle, ϕ, is shown. This asymmetric loading has the potential to exceed the gust loads of a typical gust ($\phi = 0°$) by exciting asymmetric rigid-body modes and producing an effective delay between the left and right wing excitations.

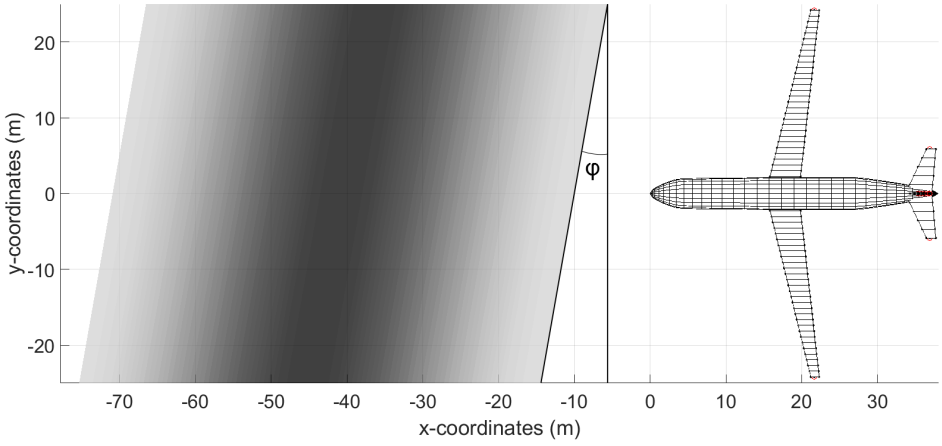

Figure 2: An asymmetric (oblique) gust profile additionally considered in this analysis, where ϕ is defined as the oblique gust angle. Darker grey denotes a larger vertical gust component.

2. *Surrogate Modelling of the Gust Loads Process*

It is clear from previous work and the literature that next-generation high-aspect ratio commercial aircraft will require the use of nonlinear solutions in order to analyse them correctly. Furthermore, a large number of additional gust types may be required in order to satisfy manufacturer and regulatory body loads criteria that some unusual gust excitation may not exceed the loads predicted by a traditional approach. Together, this results in what could potentially amount to a huge number of simulations, and extensive computational work.

In order to reduce potentially high calculation costs, a surrogate-model-based gust loads process is outlined here. A flowchart of the gust loads process is shown in Fig. 3.

In this approach, the test case to be analysed is defined, and the properties loaded into the gust loads process. The aircraft is first trimmed using pitch angle and elevators, and the equations of motion are linearised about this trim condition. A Monte Carlo simulation (MCS) using a Latin hypercube sampling (LHS) of 500 possible gust excitations (gust gradient, H, and gust oblique angle, ϕ), is defined and run using the linear system. By using the linear system, combined with model reduction techniques, the entire MCS can be computed relatively rapidly as compared to the full nonlinear approach. The maximum and minimum loads are then calculated for each case from the whole time history.

Once the gust loads envelopes are produced, a neural network is then fitted to the MCS data to produce surrogate models which can quickly and efficiently map from gust excitation parameters to maximum gust loads. With this surrogate model, an optimiser can easily determine the particular excitation which would maximise the loads.

Further work would consider more variables in the gust loads analysis than were used in this case. For example, different flight and mass cases could be included in this approach, as well as span-wise gust distributions, without any considerable increase in complexity of the problem.

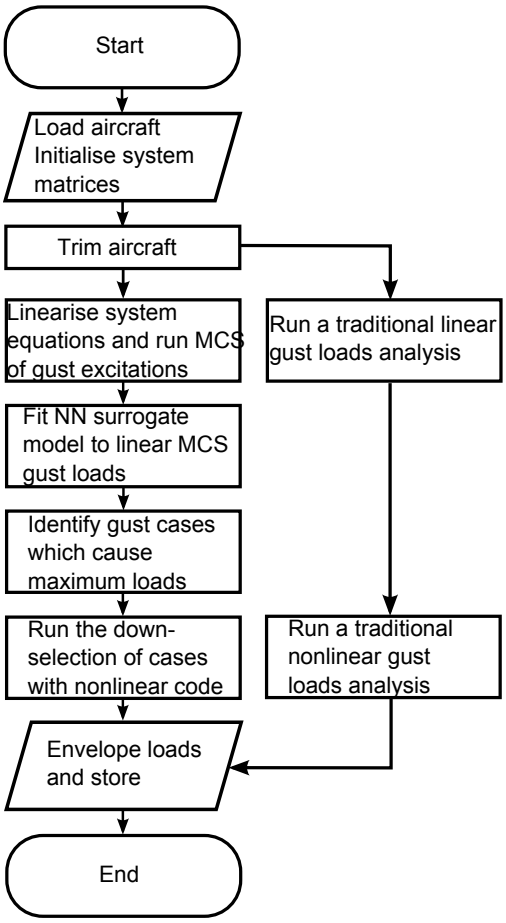

Figure 3: Flowchart of the gust loads process used in this work.

C. Uncertainty Quantification

The aim of this work is to understand how uncertainty in model parameters affect certain output IQs. Uncertainties could arise from environmental properties such as air density or temperature uncertainties, or structural properties such as stiffness, mass or damping properties which are not known exactly. It is therefore assumed that uncertain inputs to the gust loads process are known only as a probability density function (PDF) rather than as an exact value.

Determining how uncertain input parameters affect the output uncertainties can be achieved through an MCS which runs large numbers of simulations with input variables selected from a Latin hypercube sample

from an appropriate distribution. Despite the development of an efficient gust loads process in this work, it is still not possible to run enough of them to be able to extract meaningful statistical data within a realistic time frame. As such, a polynomial chaos (PC) based method is used, which uses high-order shape functions to predict how input probability density functions (PDFs) map through a black-box process to the output PDFs.

III. Test Case Definition

In this work, a representative next-generation, high-aspect-ratio, commercial aircraft is analysed. This aircraft has an aspect-ratio of 18, and the internal structural model has been generated through a sizing process to ensure wing box sections of the wing are sufficiently thick to withstand stresses of static manoeuvres, while minimizing weight (a more detailed description of this process is documented in Calderon *et al*[17]). An illustration of this aircraft can be seen in Fig. 4, and more information on the global properties of the aircraft can be seen in Tab. 1.

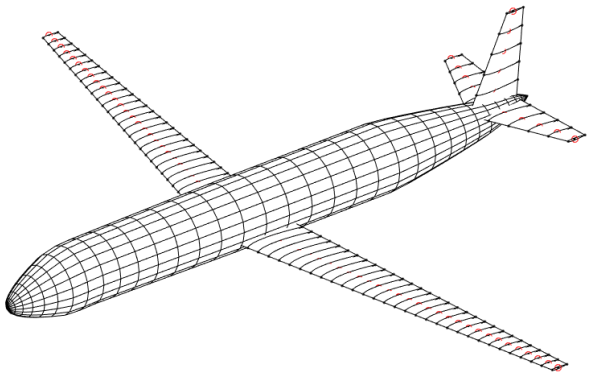

Figure 4: A rendering of the high-aspect ratio passenger aircraft (aspect-ratio 18) that has been used in this work.

	Wing	HTP	VTP
$\frac{1}{4}$ Chord Sweep (°)	12	20.6	20.6
Taper Ratio	0.25	0.35	0.35
Dihedral (°)	0	0	0
Surface Area (m^2)	130	28	28
Aspect Ratio	18	5	5
Root Thickness-Chord Ratio	0.16	0.15	0.15
Tip Thickness-Chord Ratio	0.11	0.15	0.15

Table 1: Tabulated aircraft properties.

One flight and mass case are considered in this work; the aircraft flies at Mach 0.7 at an altitude of 10,000m, and the mass case is a full payload with half fuelmass. The total mass of the aircraft in this configuration is around 69,400kg, with each wing weighing 9,970kg (lighter that that quoted in Calderon *et al*[17] due to the engines being removed for simplicity), each HTP weighing 706kg, and the VTP weighing 580kg. The remainder of the mass is distributed in the fuselage, which is considered to be rigid in these analyses. The centre of gravity for the undeformed configuration lies 2.4m behind the wing root mid-chord.

The aircraft is exposed to gust lengths in the range specified in regulations;[10,11] in this case gust lengths between 20m and 220m are used. Oblique gust angles, ϕ, will be considered between 0° (a traditionally defined gust) and 60°. Round-the-clock gusts will be considered, but a specific range need not be defined due to the fact that the worst case RTC gust orientations are first post-processed from the linear analyses, then the specific subset of cases is fed into the nonlinear simulations.

Some description of the uncertain system parameters is required to do a UQ of the gust loads process. Here, one single uncertain parameter will be considered for initial studies and to demonstrate the process, which will be an uncertainty on Young's modulus, and the associated change that this will have on the shear modulus (i.e., Poisson's ratio will be unchanged). The aircraft is sized only once for the baseline Young's modulus, and further work could consider how uncertainties propagate through the whole sizing process too, and what effect that might have.

With limited information from literature and industry about what distributions would be realistic for an uncertainty on Young's modulus, a normal distribution is selected where the mean value, μ, is equal to the baseline Young's modulus. The standard deviation, σ, is defined as $3.\bar{3}\%$ of the mean value so that approximately 99.7% (3σ) of the input cases fall between $\pm 10\%$ of the baseline value.

IV. Results

The results of the uncertainty quantification analysis is presented in this section. First, the polynomial chaos expansion method is put through a convergence study to determine the most appropriate choice of expansion order and number of samples required. After that, the UQ of the full gust loads process is presented.

A. Polynomial Chaos Expansion Convergence Study

To perform an accurate UQ using the PCE methods, an appropriate expansion order and number of samples must be used. However, despite the expressions which indicate the bare-minimum number of cases required,[18] it is not immediately clear what settings are most appropriate, and more cases generally gives better results. A Monte Carlo simulation (MCS) is one way to easily verify this by providing fairly representative statistical properties of the output PDFs. However, it is not possible to run sufficient gust load processes to give enough information to perform such an analysis in this case; the computational cost is simply too great. As an alternative, it is feasible to run a large number of single gust cases as part of a convergence study. While this does not consider every possible gust excitation, it does give an indication of what order of PCE should be used, and how many samples are required.

An MCS consisting of 1,000 nonlinear gust loads analysis, considering only one gust gradient of 80m (with $\theta = \phi = 0°$) is run, and the root mean loads and standard deviations are calculated from this MCS and considered to be the 'true' values. The mean and standard deviations are then obtained from the PCE method, considering different orders of PCE and different numbers of samples. The convergence studies for the mean values and the standard deviations can be seen in Figs. 5 and 6, respectively. It can be seen that using a expansion order of 2 or more results in excellent approximations to the mean and standard deviations as compared to the MCS. Skewness and kurtosis are also checked for convergence, but plots are not included here.

Histograms of 1,000 gust excitations are plotted in Fig. 7, for the root loads of the aircraft used in this study, and compared to probability density functions approximated using polynomial chaos expansions of varying order, with 20 samples. It can be seen how axial force, vertical shear, bending moment and torque form fairly normal PDFs, while in-plane shear and in-plane exhibit a highly skewed distribution. Even first-order PCE are very good at replicating the normal-like distributions, but cannot replicate the more skewed distributions. A similar plot is shown in Fig 8 for a PCE of order 3 with varying numbers of samples. It can be seen that a PCE of order 3, with 10 sample points or more can easily replicate even the more complex PDF shapes. Additional numbers of samples, considering 15 and 20 samples, do show minor improvements in the fit, but any number of samples in this range could be deemed accurate enough for this study.

From this analysis, it is assumed that a polynomial chaos expansion order of 3 should give sufficient information to reliably recreate probabilistic information about the gust loads process for all load direction with 10 samples or more.

B. Uncertainty Analysis of the Full Gust Loads Process

With the necessary convergence analyses carried out, the uncertainty analysis of the full gust loads process is presented. First, the static loads from the trim analysis is presented, followed by the dynamic results from the gust process.

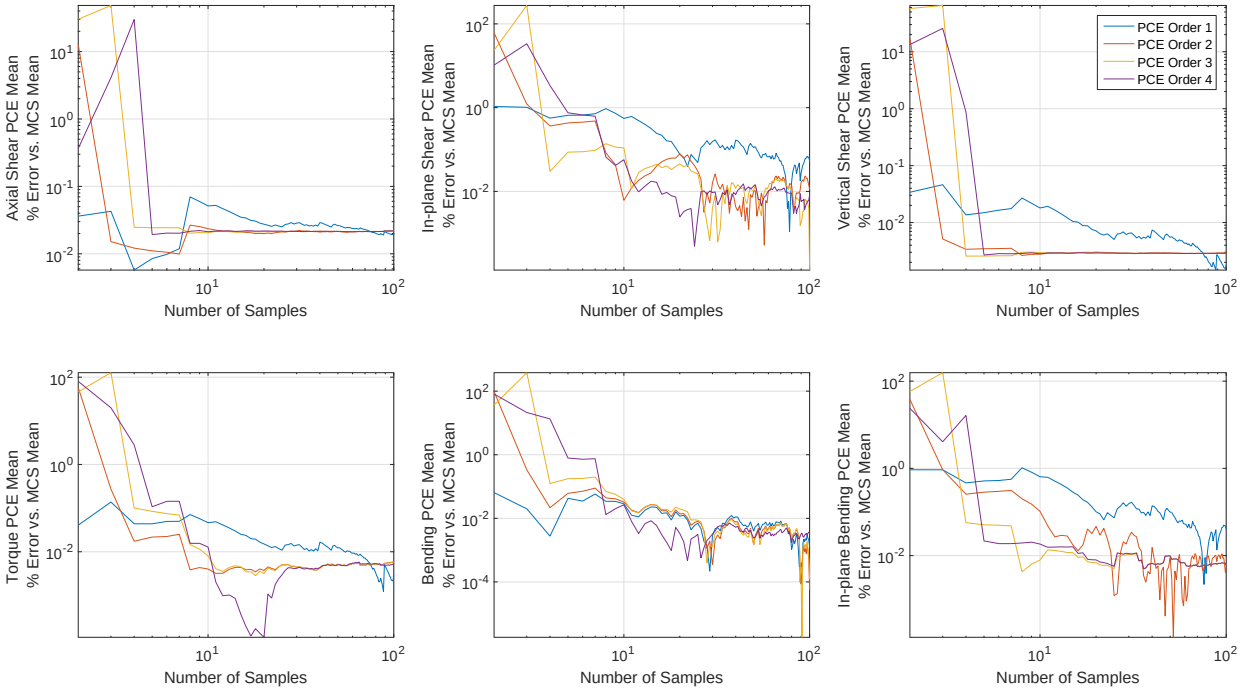

Figure 5: A convergence study of root mean loads from a nonlinear gust loads analysis compared to a Monte Carlo gust simulation with uncertain Young's modulus (1,000 cases with a gust gradient of 80m).

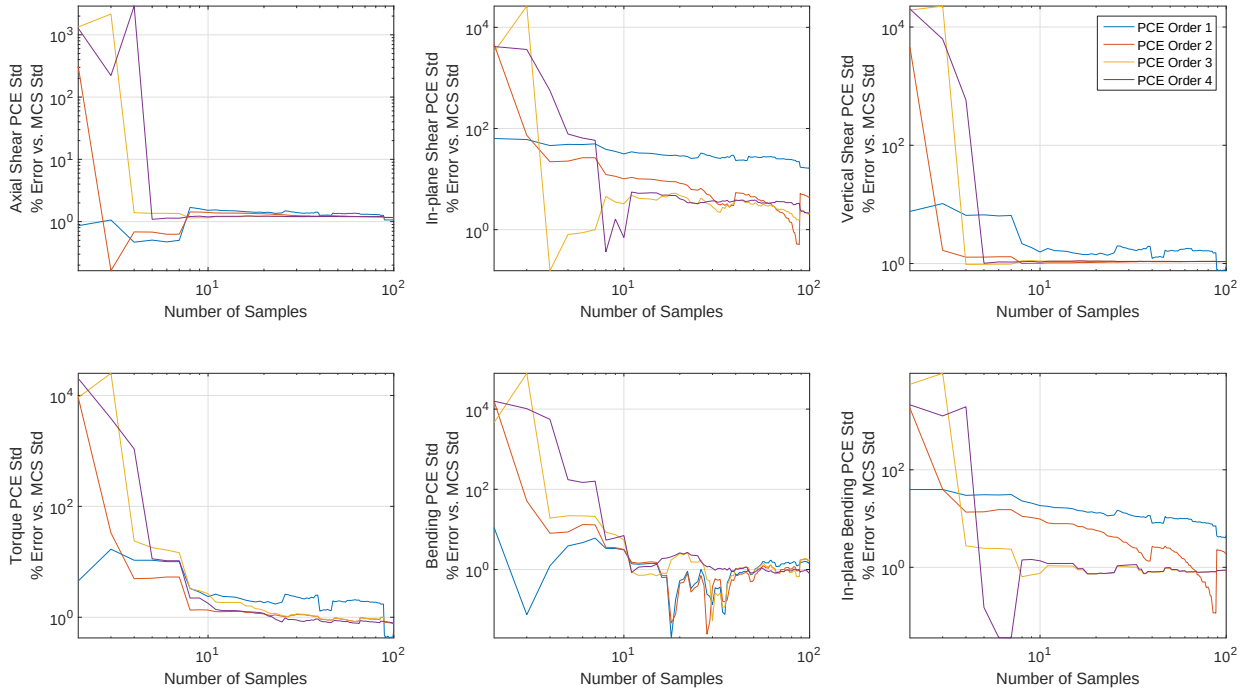

Figure 6: A convergence study of root load standard deviations from a nonlinear gust loads analysis compared to a Monte Carlo gust simulation with uncertain Young's modulus (1,000 cases with a gust gradient of 80m).

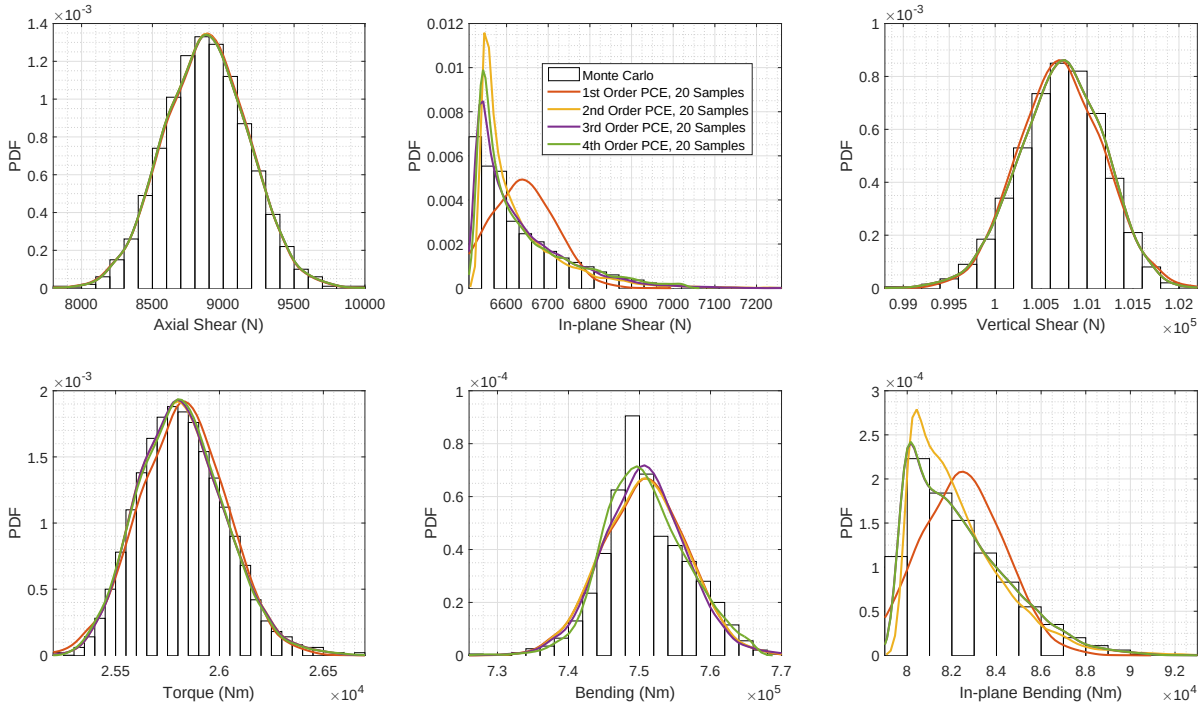

Figure 7: A histogram of a Monte Carlo gust simulation of a nonlinear gust loads analysis with uncertain Young's modulus (1,000 cases with a gust gradient of 80m) vs. polynomial chaos approximations of varying order with 20 samples.

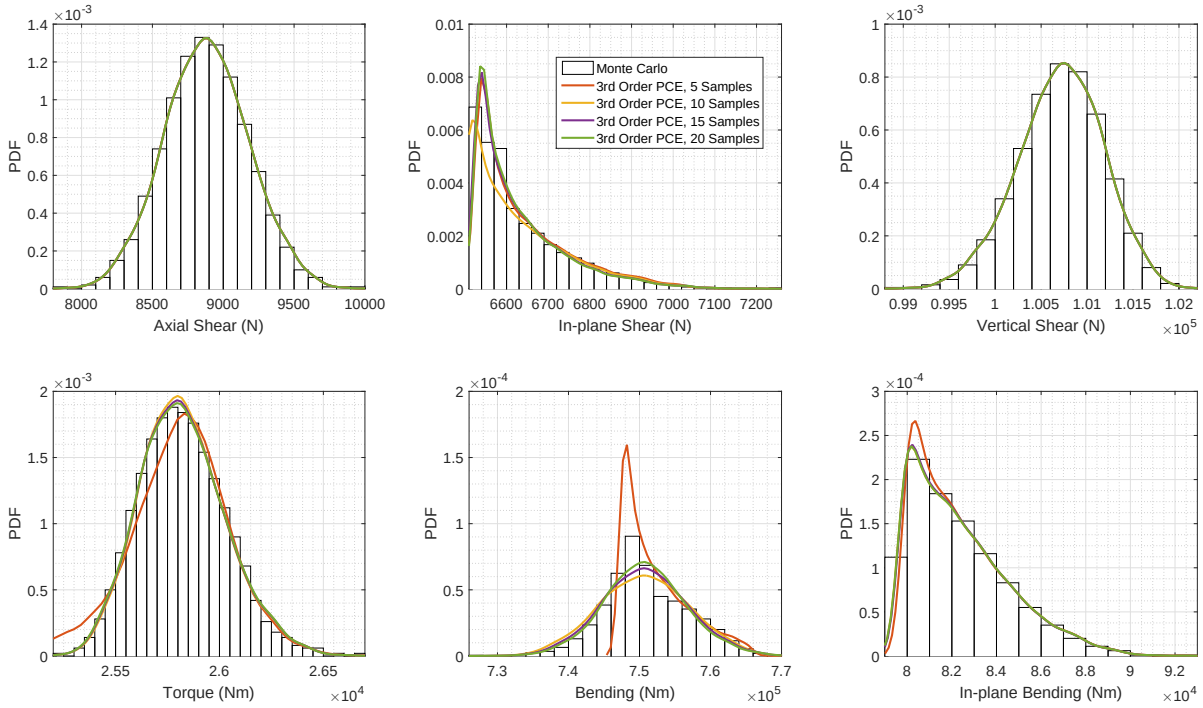

Figure 8: A histogram of a Monte Carlo gust of a nonlinear gust loads analysis simulation with uncertain Young's modulus (1,000 cases with a gust gradient of 80m) vs. polynomial chaos approximations of order 3 with various numbers of samples.

The mean angle of attack spanwise distribution on the wing at trim is plotted in Fig. 9, along with a shaded area representing the error bounds which encompass approximately 99.7% of the results. It can be seen how the uncertainty bounds are highest on the in-board and out-board sections of the wing but drop to zero mid-wing, at around 12m out-board. This uncertainty drop in the mid-wing section occurs at the rigid trim angle of attack; once flexibility effects are taken into account the root angle of attack is larger than the rigid trim angle of attack, and the outboard angle of attack is less. Since the geometry and mass remain unchanged, and hence the rigid body trim condition would also not change, the result is a point mid-wing which interestingly always has the same angle of attack regardless of wing stiffness.

The mean loads spanwise distributions for the static trim case are plotted in Fig. 10, with the same error bounds as in Fig. 9. It can be seen that uncertainty in Young's modulus has little effect on the loads, apart from in the axial force of the beam (the shaded area for other loads are barely visible) - an observation which is consistent with previous work.[8] So despite the stiffness of the wing changing by a significant factor, the displacements and orientations of the wing also change by the near inverse of the same factor and therefore for the resulting loads this factor essentially cancel. This explains why loads uncertainties are so low, yet the local angle of attack distributions are more sensitive (they are more of a geometrical IQ). Axial loads are affected more than any other load because they are driven by the in-board component of local lift, which is itself dependent on geometric shape of the wing.

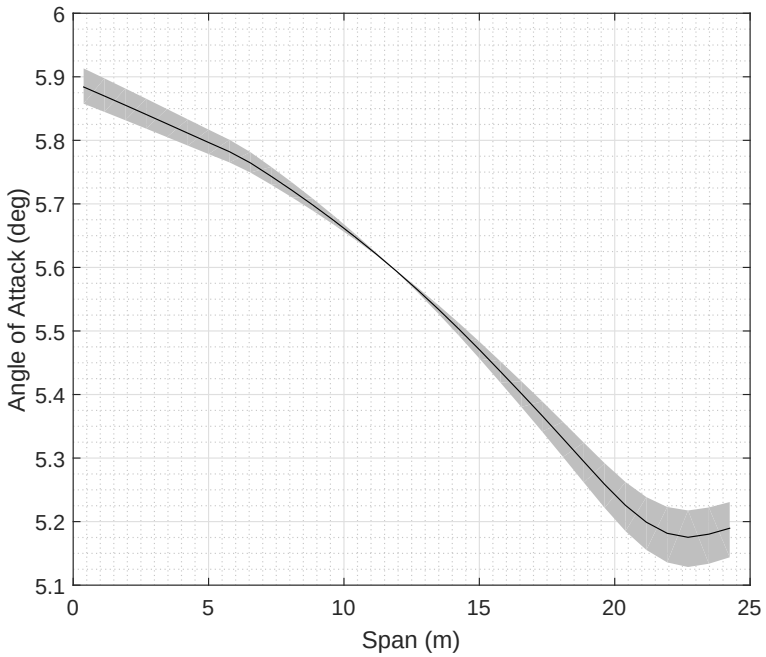

Figure 9: Mean local trim angle of attack distribution with uncertainty bounds encapsulating ≈99.7% of the possible values plotted as a shaded area.

Once a Latin hypercube analysis has been carried out on the linear system, and the loads time histories are enveloped, a neural network is fitted to the data. It was found that a simple, feed-forward neural network with one hidden layer of 25 neurons was sufficient to recreate the loads of aircraft. It can be seen in Fig. 11 how the Monte Carlo analysis compares to a surface recreated from a neural network for the root bending for one of the Monte Carlo simulation outputs. The match is generally very good, and correlation checks ensure that the match between the the MC analysis and the neural network is acceptable. It can be seen how the worst case gust excitation, in this case, is due to a traditional, vertical gust ($\phi = 0°$), with a gust gradient of around 80m. This process is repeated for all loads for all elements of the finite element problem to obtain the cases that exhibit the largest loads. Note that the RTC gust angle is not included here, and is a post-process of the linear analysis; the RTC gust angle must be output from this analysis as an additional gust case to run in the full nonlinear analysis.

A subset of cases is obtained by maximising the outputs of the surrogate model by determining the worst

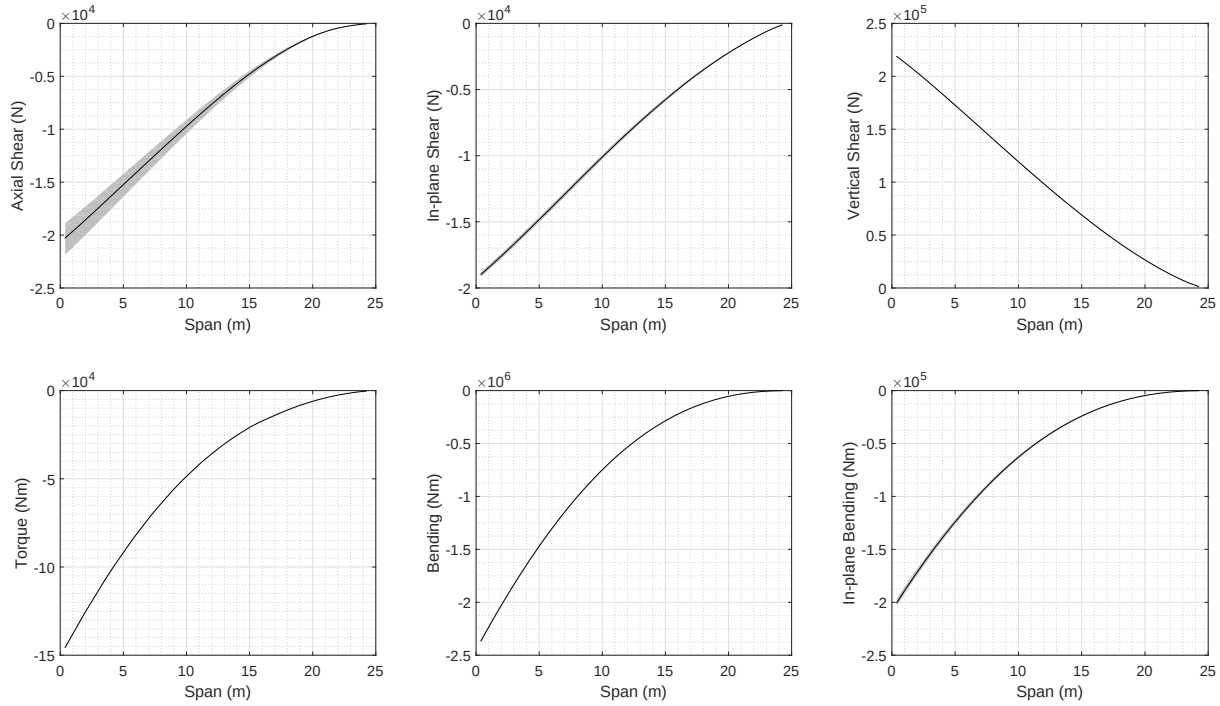

Figure 10: Mean trim loads distributions with uncertainty bounds encapsulating ≈99.7% of the possible values plotted as a shaded area.

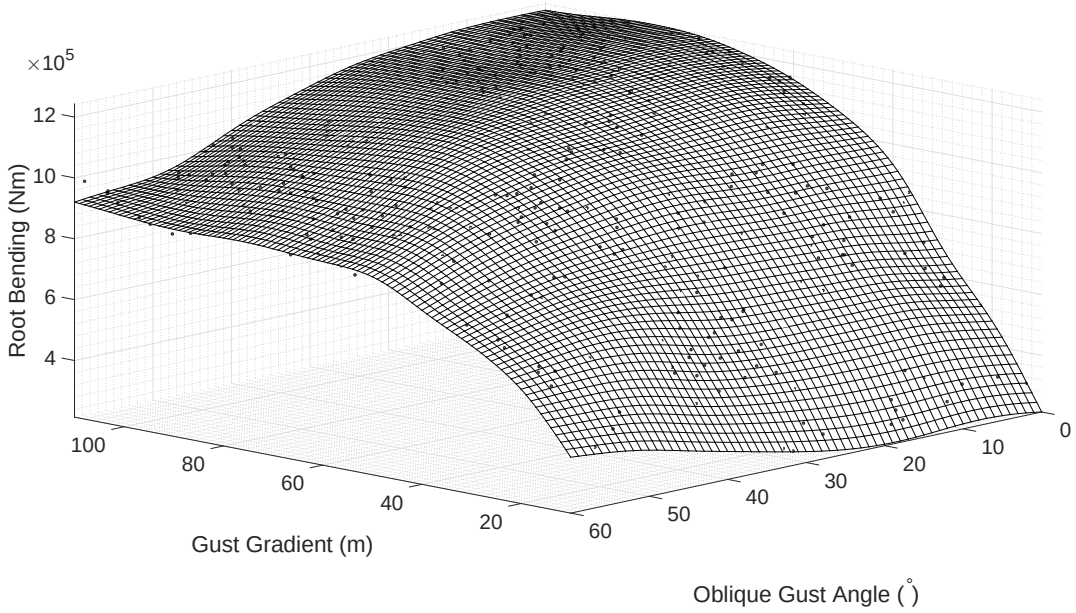

Figure 11: A comparison of the root bending moment from a Latin hypercube sample (scattered black dots) vs. a neural network derived surrogate surface.

case gust input parameters, an example is shown in Fig. 12 (the RTC gust angle, θ, is a post-process from the linear analysis). For this particular case, it can be seen how the whole problem space of potential cases can be drastically down-selected to 67, and avoids the necessity to run a fine enough resolution of all possible combinations of gust excitation in the problem space.

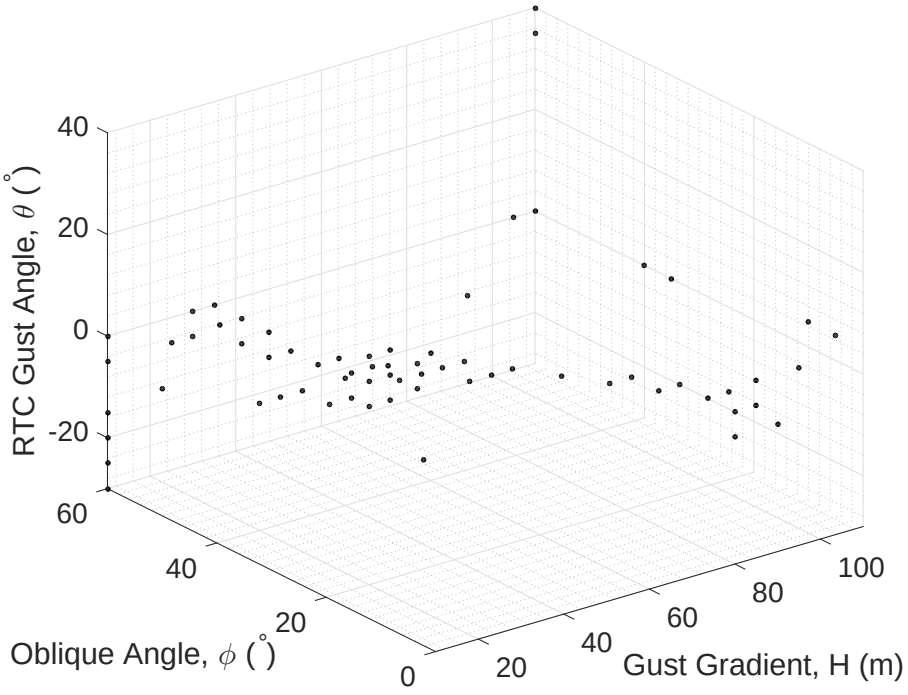

Figure 12: A scatter plot of worst case gust cases obtained from the optimisation of the surrogate model, rounded to the nearest 5 units (degrees or metres).

Mean incremental gust loads envelopes (maximum and minimum gust loads minus 1g loads) from the UQ analysis are plotted in Fig. 13, comparing a traditional 1MC gust loads analysis with the gust loads analysis carried out on the reduced set of cases including oblique gusts. The latter gust loads process can be seen to be greater or equal to the envelope of the traditional gust case, particularly in axial force, in-plane shear, bending, and torque. This can be attributed to loading on the aircraft due to oblique gust cases which exacerbates these predominantly asymmetric wing loads. A small exceedance can also be seen on the outboard sections of the wing in vertical shear and bending, where short, oblique gusts hit the outboard wing first and cause a critical gust loading. The percentage difference between the traditional gust loads process and the maximised surrogate model can be seen in Fig. 14, indicating more clearly how the maximum and minimum loads from the maximised surrogate model exceed the loads from the traditional gust loads process by a considerable amount. Both maximum and minimum torque loads from a gust loads analysis that include oblique gusts exceed the traditional envelope by 10-15% at the root, increasing to 35% outboard. Vertical shear and bending moment loads exhibit loads exceedences outboard from the oblique gusts which are over 60% of the traditional approach. This effect highlights how gust cases that would not ordinarily feature in a traditional gust loads process can become critical excitations, and that the gust loads process outlined in this paper was able to identify them.

Further to the mean values from the UQ analysis, error bounds are also included in Fig. 13 as a shaded area which approximately encompasses 99.7% (3σ) of the possible outputs. However, as seen in the trim loads in Fig. 10, uncertainties in Young's modulus has little effect on the loads of a fairly stiff aircraft such as the test case used in this work, so the error bounds are hard to see, apart from on axial and in-plane shear loads. Standard deviation distributions are plotted in Fig. 15 to illustrate more clearly how the standard deviation distributions look for the aircraft. Inclusion of atypical results does not notably affect the standard deviation of the loads as compared to those from a traditional loads process.

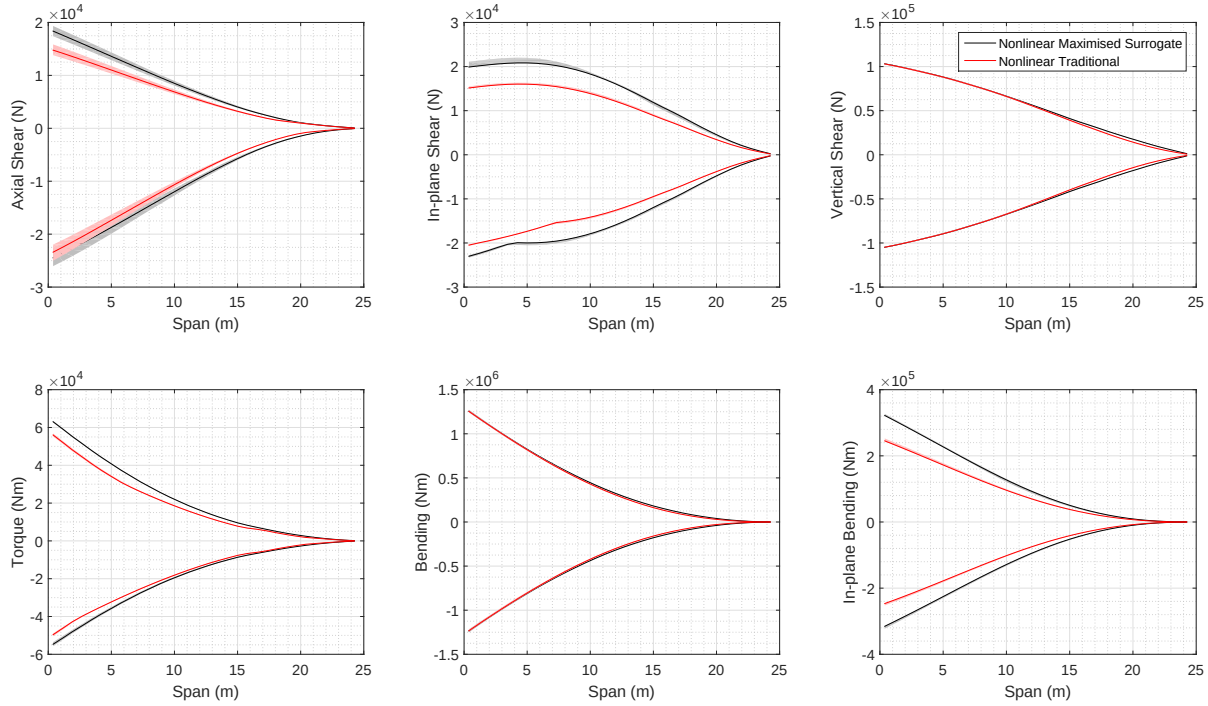

Figure 13: Mean incremental loads envelope distributions with uncertainty bounds encapsulating ≈99.7% of the possible values.

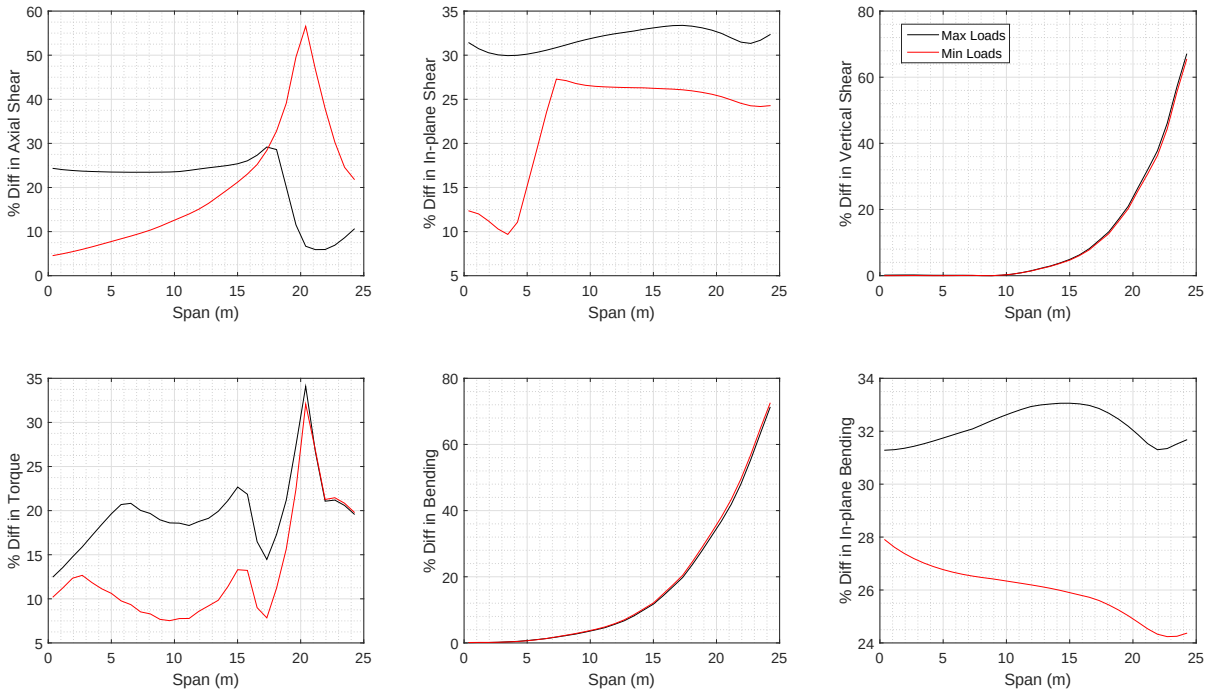

Figure 14: Percentage difference between the maximised surrogate model mean incremental gust loads presented in this work and a traditional gust loads envelope.

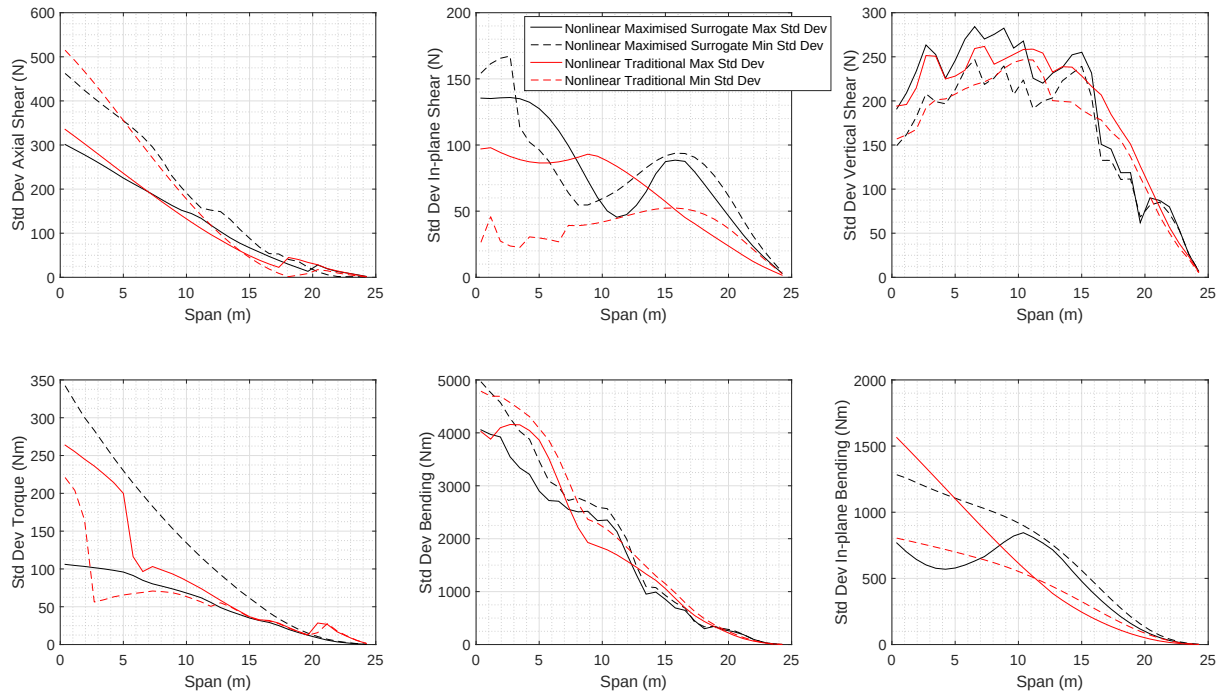

Figure 15: Standard deviation of the incremental loads envelope distributions.

V. Conclusions

An uncertainty quantification process has been presented for analysis of an aircraft exhibiting geometric structural nonlinearities. Linear approximations to the nonlinear system equations are used to build neural network-based surrogate models of the gust loads process, and select a subset of cases to run using the full nonlinear code. Polynomial chaos expansion techniques are then used on a small number of gust loads processes to determine how input uncertainties propagate through the analysis.

Convergence studies of the PCE methods show how the statistical properties of some root loads on the aircraft could be accurately recreated with only one or two expansion terms and a low number of sample cases, as compared to a Monte Carlo simulation of 1,000 cases. However, in-plane loads showed a considerably skewed distribution, and it was found that a 3rd order expansion with 10 sample cases is capable of predicting comparable statistical properties as the MCS. This approach represents a considerably more efficient way to determine output uncertainties than an MCS.

Uncertainty quantification on the trim conditions show the propagation of structural property uncertainties through the static loads process. It was seen how geometric outputs, in this case local angle of attack distribution, can exhibit a significant variance due to input uncertainties. Conversely however, loads distributions are barely affected by uncertainties in Young's modulus, apart from in axial loading where the uncertainties are relatively large. This can be attributed to the fact that axial loads are largely driven by the trim geometry.

With trim solutions found, a Monte Carlo simulation is carried out on the system linearised about the trim geometry, and a neural network surrogate model is formed mapping from gust excitation to the loads envelope. It was shown how a simple neural network with one hidden layer of 25 neurons is sufficient to predict maximum and minimum loads for the aircraft, and to produce a very low-order surrogate model of the gust loads process. Once the inputs to the surrogate were found which maximised the outputs, a subset of gust cases was identified that could exceed a loads envelope produced from a traditional gust loads analysis. An increase in root torque of the order on 10-15%, and relatively significant outboard loading in vertical shear and bending moment justified the need to include additional gust cases into the gust analysis. However, as seen in the static loads, there was little effect on the output loads variance due to structural property input uncertainties, apart from in axial and in-plane loads.

Future work will build on the work in this paper to consider additional gust loads excitations. Span-wise distributions have been previously considered in the literature, and deemed to be important for gust loads analysis of highly flexible aircraft. Such span-wise distributions would be easily included into the current methodology subject to a suitable parameterisation which still represents a physically realistic gust. Furthermore, additional sources of uncertainties could also be included simply into this approach, as well as multiple mass and flight cases.

Acknowledgments

The research leading to these results has been supported by the Agile Wing Integration Innovate UK Aerospace Technology Institute (ATI) project and the AEROGUST project (funded by the European Commission under grant agreement number 636053).[19]

The partners in AEROGUST are: University of Bristol, INRIA, NLR, DLR, University of Cape Town, NUMECA, Optimad Engineering S.r.l., University of Liverpool, Airbus Defence and Space, Dassault Aviation, Piaggio Aerospace and Valeol.

References

[1]Flightpath 2050 Europe's Vision for Aviation: Report of the High Level Group on Aviation Research. Technical Report EUR 098 EN, European Commission, 2011.

[2]H. Khodaparast, G. Georgiou, J. E. Cooper, Riccobene L., S. Ricci, G. A. Vio, and P. Denner. Efficient Worst Case "1-cosine" Gust Loads Prediction. In *15th International Forum on Aeroelasticity and Structural Dynamics*, number IFASD-2011-048, Paris, France, 2011.

[3]R. Cook, D. Calderon, E. Coetzee, J. Cooper, M. Lowenberg, and S. Neild. Worst Case Gust Prediction of Highly Flexible Wings. In *58th AIAA/ASME/ASCE/AHS/ASC structures, structural dynamics, and materials conference*, number AIAA Paper No. 2017-1355, Grapevine, Texas, 2017.

[4]D. H. Hodges. A mixed variational formulation based on exact intrinsic equations or dynamics of moving beams. *International Journal of Solids and Structures*, 26(11):1253–1273, 1990.

[5]D. H. Hodges, X. Shang, and C. E. S. Cesnik. Finite element solution of nonlinear intrinsic equations for curved composite beams. *Journal of the American Helicopter Society*, 41(9), 1996.

[6]J. G. Leishman. Unsteady lift of a flapped airfoil by indicial concepts. *Journal of Aircraft*, 31(2):288–297, 1994.

[7]W. P. Jones. Aerodynamic forces on wings in nonuniform motion. *ARCR & M 2117*.

[8]R. G. Cook, C. J. A. Wales, A. L. Gaitonde, D. P. Jones, and J. E. Cooper. Uncertainty quantification in gust loads analysis of a highly flexible aircraft wing. In *International Forum on Aeroelasticity and Structural Dynamics*, Como, Italy, 2018.

[9]C. M. Shearer and C. E. S. Cesnik. Modified Generalized-α Method for Integrating Governing Equations of Very Flexible Aircraft. In *47th AIAA/ASME/ASCE/AHS/ASC Structures, Structural Dynamics, and Materials Conference*, number AIAA 2006-1747, Newport, Rhode Island, 2006.

[10]FAA Federal Aviation Regulations, Section 25.341. `https://www.faa.gov/regulations_policies/advisory_circulars/index.cfm/go/document.information/documentID/1024906`. Accessed: 2017-12-05.

[11]European Aviation Safety Agency (EASA). *CS-25 Certification Specifications for Large Aeroplanes*. 2003.

[12]T. L. Lomax. *Structural Loads Analysis: Theory and Practice for Commercial Aircraft*. American Institure of Aeronautics and Astronautics, Reston, Virginia, USA, 1996.

[13]Special Conditions: Airbus Model A380-800 Airplane, Discrete Gust Requirements. Vol. 71, No. 15. Technical Report 14 CFR Part 25 [Docket No. NM316; Special Conditions No. 25-312-SC], Federal Aviation Administration, January 24th 2006.

[14]J. C. Houbolt and A Sen. Cross-spectral Functions based on von Karman's Spectral Equation. Technical Report NASA CR-2011, National Aeronautics and Space Administration, March 1972.

[15]J. C. Houbolt. Effect of Nonuniform Spanwise gusts on Aircraft Vertical Response. Technical Report AFOSR TR-74-054, United States Air Force, January 1974.

[16]Broad Agency Announcement (BAA) Vulture II Appendices. Technical Report DARPA-BAA-10-04, DARPA, 16th October 2009.

[17]D. E. Calderon, J. E. Cooper, M. Lowenberg, S. A. Neild, and E. B. Coetzee. On the Effect of Including Geometric Nonlinearity in the Sizing of a Wing. In *59th AIAA/ASCE/AHS/ASC Structures, Structural Dynamics, and Materials Conference*, Kissimmee, Florida, 2018.

[18]D. Xiu and G. E. Karniadakis. The Wiener-Askey Polynomial Chaos for Stochastic Differential Equations. *SIAM Journal on Sxientific Computing*, 24(2):619–644, 2002.

[19]AEROGUST project (funded by the European Commission under grant agreement number 636053). `https://www.aerogust.eu`. Accessed: 2017-05-26.